ISSN : 0974 - 7486 Volume 10 Issue 8

Materials Science

An Indian Journal

Full Paper

MSAIJ, 10(8), 2014 [320-328]

Structural, electrical, mechanical and soldering properties of new proposed Tin-Zinc-Cadmium lead free solder alloys

Abu Bakr El-Bediwi*, N.A.El-Shishtawi, Aia Abd El-Baset
Metal Physics Lab., Physics Department, Faculty of Science, Mansoura University, (EGYPT)
E-mail : Baker_elbediwi@yahoo.com

ABSTRACT

The aim of present work was to produce new Sn-Zn-Cd alloy with superior soldering properties. Microstructure, electrical resistivity, elastic modulus, internal friction, thermal diffusivity, hardness, melting point, pasty range and wettability of $Sn_{91}Zn_{9-x}Cd_x$ (x= 0, 1.5, 3, 5 wt.%) and $Sn_{86}Zn_4Cd_{10}$ rapidly solidified alloys have been investigated. Melting point, contact angle and elastic modulus values of $Sn_{91}Zn_{9-x}Cd_x$ alloy decreased but electrical resistivity, internal friction and pasty range values increased with increasing cadmium content. The $Sn_{86}Zn_4Cd_{10}$ alloy has the beast soldering properties for electronic application.

KEYWORDS

Microstructure;
Melting point;
Contact angle;
Elastic modulus;
Hardness;
Pasty range;
Internal friction and thermal diffusivity;
Sn-Zn-Cd alloy.

INTRODUCTION

Sn—Zn solder alloy containing about 9 wt % zinc (eutectic composition) has been proposed as a lead-free solder material which is expected to be put into practical use for reflow soldering. Further, an Sn—Zn solder alloy containing about 8 wt % zinc and 1 to 3 wt % bismuth has been also proposed. Those Sn—Zn solder alloys have advantages such that a eutectic temperature of a tin-zinc alloy is equal to 199° C closest to a eutectic point of a tin-lead alloy among Sn-based lead-free solder alloys, and costs of raw materials of them are lower than those of the other lead-free solder alloys. Lead-free solders having high performance and many studies have been made on various alloy-system solders based on Sn, e.g., Sn-9Zn, Sn-3.5Ag, Sn-3Ag-0.5Cu, etc. as likely substitutes[1-3]. Also the dependence of frequency over a range of 0-3 Hz on Young's modulus and internal friction in Sn-9Zn and Sn-3.5Ag eutectic lead free solder alloys was investigated by T. Ohoak et al[4]. The progress made in the properties of two lead free solder alloys, Sn-3.5%Ag-1%Zn and Zn-In, are described by M. Mc Cormack et al[5]. Solidification behaviors of Sn-9Zn-XAg lead-free solder alloys are examined by using scanning electron microscopy, electron prope microanalysis, X-ray analysis, computer aided-cooling curve analysis and differential scanning calorimetry[6]. A review on the microstructure and mechanical properties of Sn-58Bi, Sn-52In and Sn-3.4Ag lead free solder alloys are reported by Glazer[7]. Several papers[8-10] show that, the eutectic Sn-3.5%Ag is regarded as a good lead free solder alloy for certain aspects such as superior fatigue properties[11]. Effects of indium addition on solidus and liquidus temperatures, wetting time, wetting force, tensile strength and microhardness of Sn-0.3Ag-0.7Cu lead-free solder alloy were investigated[12]. Structure, electrical resistivity, wettability, melting point and elastic modulus of 50Sn-50In, 72.2Sn-20In-2.8Ag,72.5Sn-25In-2.5Ag and 95Sn-5Ag lead free solder alloys have been investigated[13]. The aim of this work is to produce new alloy with superior soldering properties by adding cadmium to tin- zinc alloy.

EXPERIMENTAL WORK

In the present work, $Sn_{91}Zn_{9-x}Cd_x$ (x= 0, 1.5, 3, 5 wt.%) and $Sn_{86}Zn_4Cd_{10}$ were melted in a muffle furnace using tin, silver and cadmium of purity better than 99.5 %. The resulting ingots were turned and re-melted four times to increase the homogeneity. From these ingots, long ribbons of about 4 mm width and ~70 μm thickness were prepared by a single roller method in air (melt spinning technique). The surface velocity of the roller was 31.4 m/s giving a cooling rate of $\sim 3.7 \times 10^5$ K/s. The samples then cut into convenient shape for the measurements using double knife cuter. Microstructure of used samples was performed on the flat surface of all samples using an Shimadzu X–ray Diffractometer (Dx–30, Japan) of Cu–Kα radiation with λ=1.54056 Å at 45 kV and 35 mA and Ni–filter in the angular range 2θ ranging from 0 to 100° in continuous mode with a scan speed 5 deg/min. The electrical resistivity was measured by a conventional double bridge method. The differential thermal analysis (DSC) thermographs were obtained by Shimadzu DTA-50 with heating rate 10 k/min in the temperature range 300-470 °k. All the samples have the same mass, which is 2 mg. The internal friction Q^{-1} and the elastic constants were determined using the dynamic resonance method. The value of the dynamic Young modulus *E* is determined by the following relationship[14–16]:

$$\left(\frac{E}{\rho}\right)^{1/2} = \frac{2\pi L^2 f_0}{kz^2}$$

Where ρ the density of the sample under test, L the length of the vibrated part of the sample, k the radius of gyration of cross section perpendicular to its plane of motion, f_0 the resonance frequency and *z* the constant depends on the mode of vibration and is equal to 1.8751. From the resonance frequency f_0 at which the peak damping occurs, the thermal diffusivity, D_{th}, can be obtained directly from the following equation:

$$D_{th} = \frac{2d^2 f_0}{\pi}$$

where *d* is the thickness of the sample

Plotting the amplitude of vibration against the frequency of vibration around the resonance f_0 gives the resonance curve, the internal friction, Q^{-1}, of the sample can be determined from the following relationship:

$$Q^{-1} = 0.5773 \frac{\Delta f}{f_0}$$

Where Δf the half width of the resonance curve

RESULTS AND DISCUSSION

X-ray analysis

X-ray diffraction patterns of quenched $Sn_{91}Zn_{9-x}Cd_x$ (x= 0, 1.5, 3, 5 wt.%) and $Sn_{86}Zn_4Cd_{10}$ alloys, Figure (1), show that sharp lines of body-centered tetragonal Sn and Zn very small hexagonal peaks of Zn detected by x-ray diffractometer. TABLE 1 (a, b, c, d and e) shows x-ray diffraction analysis, (2θ, Intensity, Miller indices (h, k, l), full width half maximum, (FWHM)) of quenched $Sn_{91}Zn_{9-x}Cd_x$ (x= 0, 1.5, 3, 5 wt.%) and $Sn_{86}Zn_4Cd_{10}$ alloys. From these analysis it obvious that adding Cd content to Sn- Zn alloy caused change in its matrix microstructure such as crystallinity which is related to intensity of the peak, crystal size which is related to full width half maximum and the orientation which is related to the position of the peak, 2θ.

Soldering properties

Wettability

A property of importance to the manufacturing or product engineer is wettability. Indeed, wettability is defined as the tendency for a liquid metal to spread on a solid surface. Wettability is the precursor of solder ability, which describes the solder's ability to form an actual joint on a circuit board. Wettability is quantitatively assessed by the contact angle formed at the solder substrate's flux triple point. The contact angles of quenched $Sn_{91}Zn_{9-x}Cd_x$ (x= 0, 1.5, 3, 5 wt.%) and $Sn_{86}Zn_4Cd_{10}$ alloys on Cu substrate are shown in TABLE 2. From these results, it is clear that adding Cd content to Sn- Zn alloy due a significant change in its contact angle, (wettability), and $Sn_{88}Ag_2Cd_{10}$ alloy

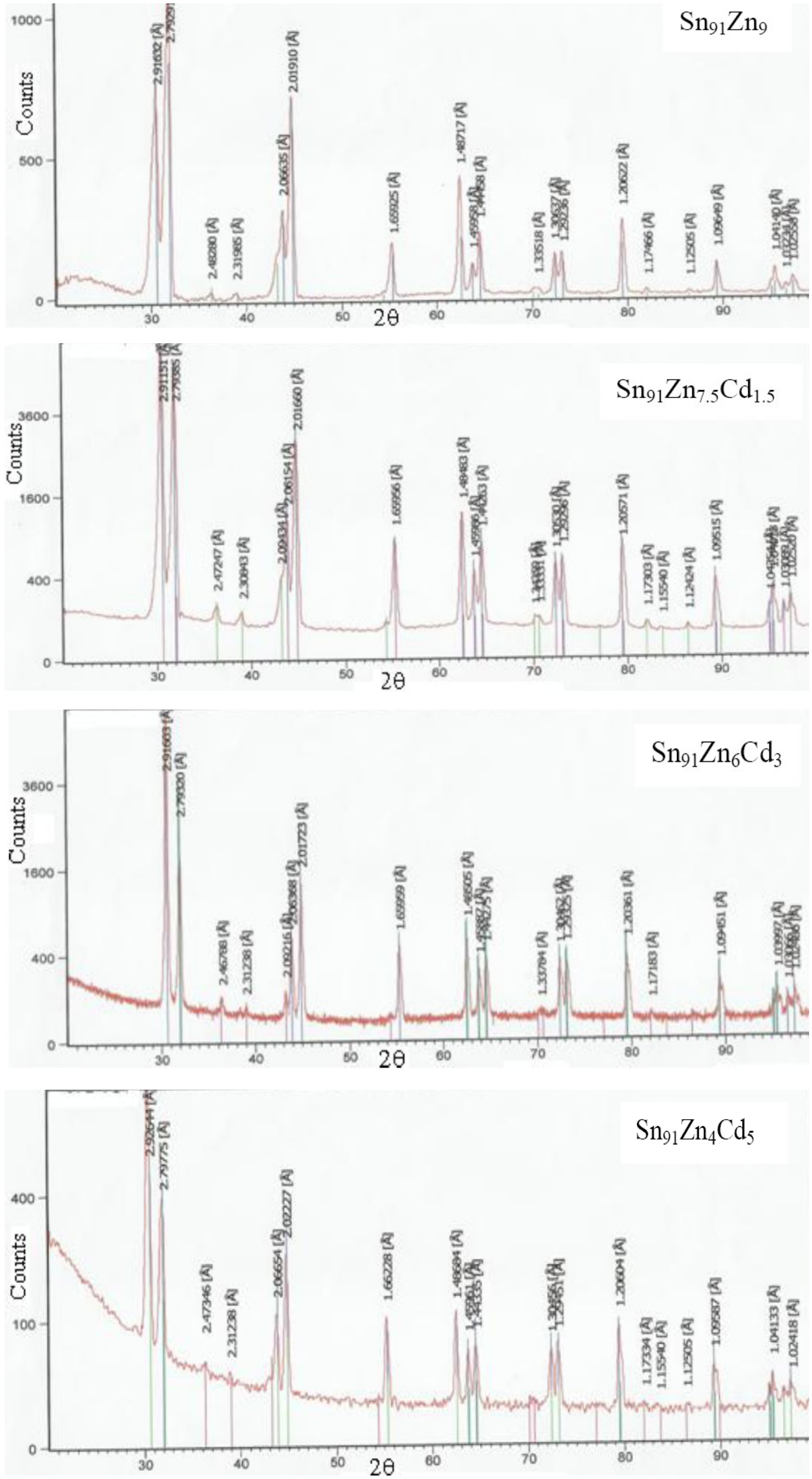
$Sn_{91}Zn_9$
Counts
2θ
$Sn_{91}Zn_{7.5}Cd_{1.5}$
Counts
2θ
$Sn_{91}Zn_6Cd_3$
Counts
2θ
$Sn_{91}Zn_4Cd_5$
Counts
2θ

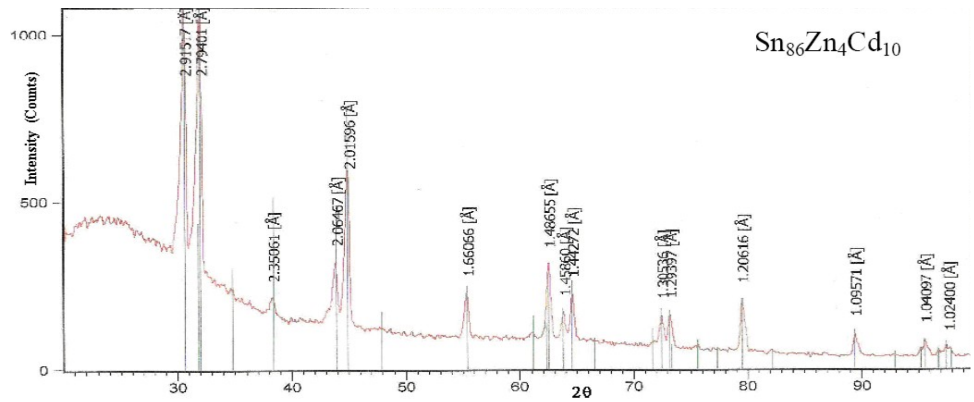

Figure 1 : X-ray diffraction patterns of Sn-Zn-Cd rapidly solidified alloys

TABLE 1 : X-ray analysis of Sn-Zn-Cd rapidly solidified alloys

a) $Sn_{91}Zn_9$

2θ	d-Å	Int%	FWHM	Phase	hkl	τÅ
30.6569	2.916	72.74	0.2755	Sn	200	298.99
32.0473	2.793	100	0.3346	Sn	101	247.02
36.1800	2.483	2.53	0.4723	Zn	002	176.95
38.8195	2.319	2.56	0.4723	Zn	100	178.34
43.8128	2.066	32.09	0.2755	Sn	220	310.792
44.8933	2.019	70.62	0.3542	Sn	211	242.67
55.3726	1.659	17.65	0.3542	Sn	301	253.28
62.4491	1.487	42.40	0.4133	Sn	112	224.77
63.7666	1.459	10.68	0.3542	Sn	400	264.13
64.5081	1.445	22.14	0.2558	Sn	321	367.22
70.5363	1.335	1.72	0.7872	Zn	110	123.60
72.3332	1.306	14.25	0.2755	Sn	420	357.18
73.2444	1.292	13.26	0.2952	Sn	411	335.30
79.4549	1.206	27.03	0.2755	Sn	312	374.92
82.0380	1.175	1.71	0.4723	Zn	112	222.93
86.5100	1.1259	2.42	0.0900	Zn	201	1211.95
89.3517	1.096	11.60	0.2755	Sn	431	405.50
95.5116	1.041	9.20	0.2755	Sn	332	428.91
96.6256	1.032	2.74	0.2362	Sn	440	505.71
97.3691	1.026	5.47	0.4800	Sn	521	250.68

b) $Sn_{91}Zn_{7.5}Cd_{1.5}$

2θ	d-Å	Int.%	FWHM	Phase	hkl	τÅ
30.7089	2.91151	97	0.2558	Sn	200	322.05
32.0361	2.79385	100	0.1574	Sn	101	525.09
36.3365	2.47247	1.87	0.4723	Zn	002	177.03
39.0194	2.30843	1.21	0.2362	Zn	100	356.82
43.1977	2.09434	6.07	0.1574	Sn	220	542.82
43.9202	2.06154	21.89	0.1968	Sn	220	435.24
44.9519	2.01660	53.85	0.1574	Sn	211	546.195
55.3613	1.65956	15.28	0.0787	Sn	301	1139.87
62.5584	1.48483	23.28	0.1181	Sn	112	787.06
63.7530	1.45986	7.08	0.3149	Sn	400	297.08
64.6059	1.44263	14.41	0.1771	Sn	321	530.698
70.6500	1.33331	0.62	0.0900	Zn	110	1081.86
72.4023	1.30530	9.21	0.1181	Sn	420	833.58
73.2044	1.29296	10.44	0.1771	Sn	411	558.75
79.4161	1.20571	12.26	0.1680	Sn	312	614.66
82.0933	1.17303	0.60	0.4800	Zn	112	219.45
86.4988	1.12424	0.28	0.5760	Zn	201	189.35
89.3963	1.09515	6.33	0.2400	Sn	431	465.66
95.1496	1.04354	1.86	0.2400	Sn	332	490.65
95.5615	1.04013	4.75	0.2400	Sn	332	492.59
96.6995	1.03089	1.85	0.2400	Sn	440	498.06
97.4170	1.02520	3.17	0.2880	Sn	521	418.003

c) $Sn_{91}Zn_5Cd_3$

2θ	d-Å	Int-%	FWHM	Phase	hkl	τÅ
30.6601	2.916	100	0.1968	Sn	200	418.56
32.0438	2.793	38.5	0.2362	Sn	100	349.92
36.4064	2.468	.87	0.3149	Zn	002	265.56
38.9500	2.312	0.27	0.0900	Zn	100	936.24
43.2448	2.092	1.51	0.1574	Sn	220	542.91
43.8725	2.064	8.55	0.0984	Sn	220	870.34
44.9370	2.017	21.99	0.2165	Sn	211	397.07
55.3602	1.659	7.52	0.1181	Sn	301	759.59
62.5482	1.485	9.72	0.1574	Sn	112	590.51
63.8013	1.459	3.78	0.2362	Sn	400	396.16
64.6002	1.443	5.31	0.2755	Sn	321	341.14
70.3752	1.338	0.18	0.2872	Zn	110	123.48
72.4459	1.305	5.05	0.1181	Sn	420	833.81
73.1853	1.293	5.34	0.0984	Sn	411	1005.52
79.5821	1.204	6.13	0.2400	Sn	312	430.78
82.1959	1.172	0.19	0.5760	Zn	112	183.02

c) $Sn_{91}Zn_5Cd_3$						
2θ	**d-Å**	**Int-%**	**FWHM**	**Phase**	**hkl**	**τÅ**
89.4632	1.095	3.15	0.2400	Sn	431	465.93
95.5813	1.039	1.85	0.2400	Sn	332	492.68
96.7286	1.031	0.89	0.1920	Sn	440	622.76
97.4608	1.025	1.55	0.2400	Sn	521	501.82
d) $Sn_{91}Zn_4Cd_5$						
2θ	**d-Å**	**Int-%**	**FWHM**	**Phase**	**hkl**	**τÅ**
30.5484	2.92644	100	0.492	Sn	200	167.38
31.9903	2.79775	43.95	0.2558	Sn	101	323.07
36.3214	2.47346	3.69	0.1212	Zn	002	689.81
38.95	2.31238	0.99	0.09	Zn	100	936.24
43.8084	2.06654	12.55	0.3149	Sn	220	271.90
44.8191	2.02227	30.35	0.3346	Sn	211	256.81
55.2631	1.66228	12.8	0.3149	Sn	301	284.75
62.4645	1.48684	13.31	0.2755	Sn	112	337.22
63.7649	1.45961	6.67	0.1771	Sn	400	528.26
64.57	1.44335	7.25	0.3542	Sn	321	265.296
72.45	1.30456	6.48	0.2165	Sn	420	454.85
73.1031	1.29451	7.36	0.3149	Sn	411	314.04
79.4686	1.20604	11.13	.2362	Sn	312	437.35
82.15	1.17334	0.28	0.09	Zn	112	1170.89
86.51	1.12505	042	0.09	Zn	201	1211.95
89.4157	1.09587	4.16	0.2558	Sn	431	436.97
95.521	1.04133	3.09	0.2165	Sn	332	545.84
97.5473	1.02418	1.36	0.576	Sn	521	209.27
e) $Sn_{86}Zn_4Cd_{10}$						
2θ	**d-Å**	**Int-%**	**FWHM**	**Phase**	**hkl**	**τÅ**
30.6694	2.915	94.14	0.2558	Sn	200	322.023
32.0343	2.794	100	0.2755	Sn	100	299.998
38.2916	2.351	7.03	0.3936	Zn	100	213.649
43.8502	2.065	24.03	0.3149	Sn	220	271.942
44.9669	2.016	55.65	0.3149	Sn	211	273.026
55.3215	1.661	17.94	0.2952	Sn	301	303.833
62.4781	1.487	29.49	0.3149	Sn	112	295.053
63.8143	1.459	10.44	0.2362	Sn	400	396.191
64.6013	1.443	18.48	0.2362	Sn	321	397.902
72.3984	1.305	11.89	0.3149	Sn	420	312.618
73.1379	1.294	12.67	0.3149	Sn	411	314.108
79.4595	1.206	20.26	0.2362	Sn	312	437.321
89.4322	1.096	8.98	0.2165	Sn	431	516.368
95.5646	1.041	6.35	0.2362	Sn	332	500.527
97.5708	1.024	3.19	0.5760	Sn	521	209.322

have adequate contact angle, leading to their spreading on the substrate.

TABLE 2 : Contact angles of quenched $Sn_{91}Zn_{9-x}Cd_x$ (x= 0, 1.5, 3, 5 wt.%) and $Sn_{86}Zn_4Cd_{10}$ alloys on Cu substrate

Alloys	Contact angle (θ)
$Sn_{91}Zn_9$	$37.13^{\circ}\pm2.216^{\circ}$
$Sn_{91}Zn_{7.5}Cd_{1.5}$	$28.25^{\circ}\pm3.379^{\circ}$
$Sn_{91}Zn_6Cd_3$	$28.5^{\circ}\pm3.15^{\circ}$
$Sn_{91}Zn_4Cd5$	$31.75^{\circ}\pm159^{\circ}$
$Sn_{86}Zn_4Cd_{10}$	30±2

Melting point and pasty range

The melting point of $Sn_{91}Zn_{9-x}Cd_x$ (x= 0, 1.5, 3, 5 wt.%) and $Sn_{86}Zn_4Cd_{10}$ alloys was measured and then seen in TABLE (3), because it is very important for industrial applications. Also thermo-graphs, Figure (2), of $Sn_{91}Zn_{9-x}Cd_x$ (x= 0, 1.5, 3, 5 wt.%) and $Sn_{86}Zn_4Cd_{10}$ alloys which have a little variations in the shape of Exo-thermal peaks, (That means a change in internal structure caused after adding Cd content) and that agrees with the results seen in x-ray diffraction analysis. The melting temperature of Sn- Zn alloy decreased after adding cadmium content as seen in TABLE 3. The $Sn_{86}Zn_4Cd_{10}$ alloy has lower melting point (179.66 °C) compared to commercial eutectic lead- tin (183 °C) solder alloy.

TABLE 3 : melting point and pasty range of quenched $Sn_{91}Zn_{9-x}Cd_x$ (x= 0, 1.5, 3, 5 wt.%) and $Sn_{86}Zn_4Cd_{10}$ alloys

Alloys	Melting point °C	Pasty range °C
$Sn_{91}Zn_9$	201.55	
$Sn_{91}Zn_{7.5}Cd_{1.5}$	195.38	16.31
$Sn_{91}Zn_6Cd_3$	194.63	16.3
$Sn_{91}Zn_4Cd5$	194.0	20.65
$Sn_{86}Zn_4Cd_{10}$	179.66	20.21

The solidus temperature is defined as the temperature at which the first deviation from the base line appears (Figure2). The deviation signals that a phase change is taking place. Thus the solidus temperature has been reached The tangent line, drawn in by the DSC, is an approximation of the solidus temperature. The liquidus temperature is defined as the temperature at which the graph returns to the baseline. The end of the deviation signifies the end of the phase change, i.e. the alloy has reached the liquid phase and the liquidus temperature. The tolerance on the values from the chart is ± 2 °C. The appearance of the DSC output is severely affected by the scan rate. Scan rate is the speed at which

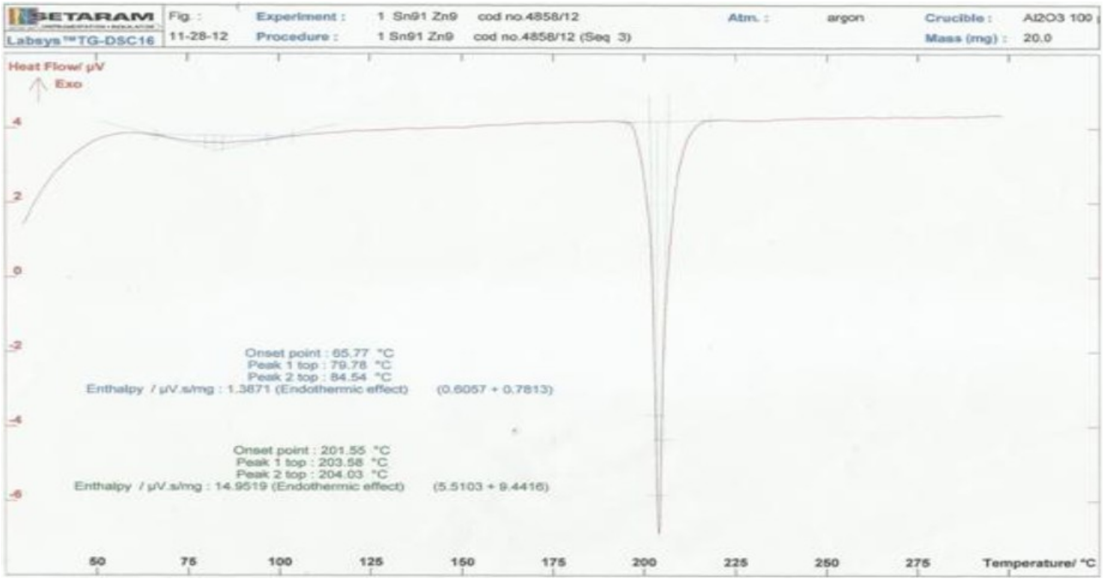
SETARAM
Labsys TM TG-DSC16
Fig. :
11-28-12
Experiment : 1 Sn91 Zn9 cod no.4858/12
Procedure : 1 Sn91 Zn9 cod no.4858/12 (Seq 3)
Atm. : argon
Crucible : Al2O3 100
Mass (mg) : 20.0
Heat Flow/ µV
Exo
Onset point : 65.77 °C
Peak 1 top : 79.78 °C
Peak 2 top : 84.54 °C
Enthalpy / µV.s/mg : 1.3871 (Endothermic effect) (0.6057 + 0.7813)
Onset point : 201.55 °C
Peak 1 top : 203.58 °C
Peak 2 top : 204.03 °C
Enthalpy / µV.s/mg : 14.9519 (Endothermic effect) (5.5103 + 9.4416)
Temperature/ °C

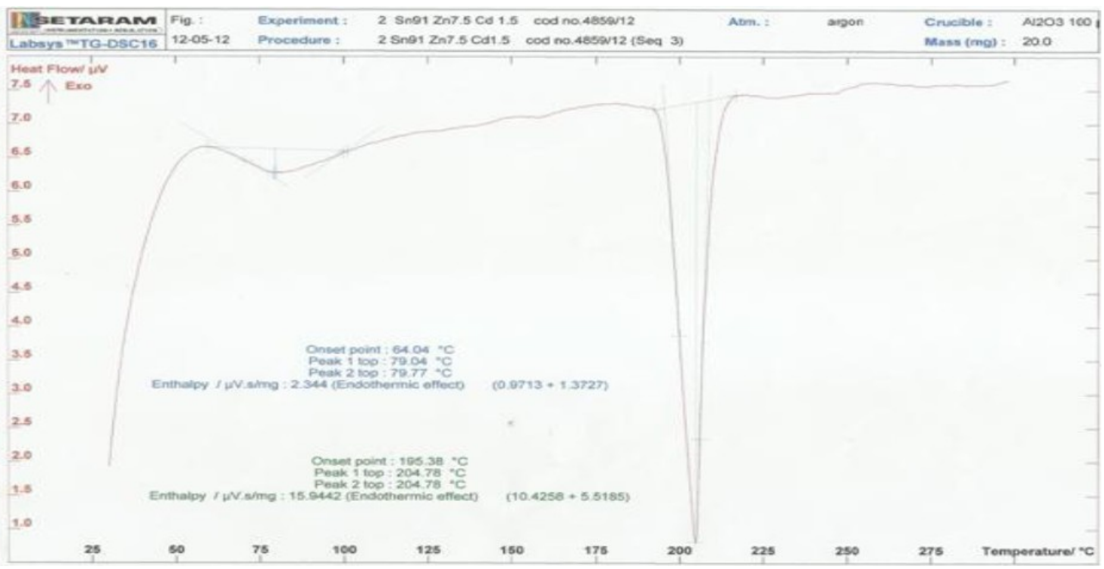
SETARAM
Labsys TM TG-DSC16
Fig. :
12-05-12
Experiment : 2 Sn91 Zn7.5 Cd 1.5 cod no.4859/12
Procedure : 2 Sn91 Zn7.5 Cd1.5 cod no.4859/12 (Seq 3)
Atm. : argon
Crucible : Al2O3 100
Mass (mg) : 20.0
Heat Flow/ µV
Exo
Onset point : 64.04 °C
Peak 1 top : 79.04 °C
Peak 2 top : 79.77 °C
Enthalpy / µV.s/mg : 2.344 (Endothermic effect) (0.9713 + 1.3727)
Onset point : 195.38 °C
Peak 1 top : 204.78 °C
Peak 2 top : 204.78 °C
Enthalpy / µV.s/mg : 15.9442 (Endothermic effect) (10.4258 + 5.5185)
Temperature/ °C

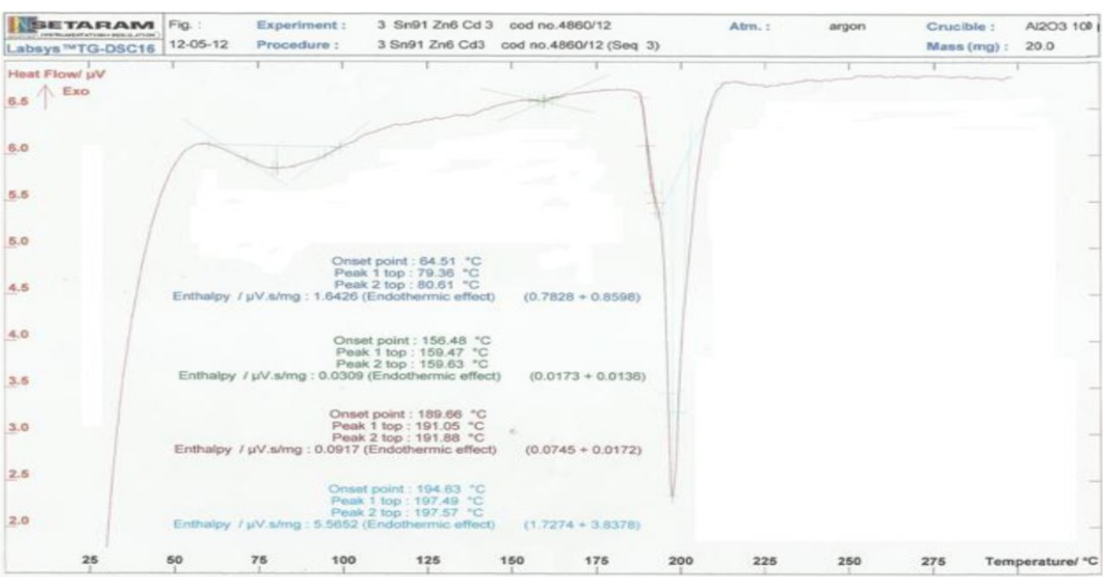
SETARAM
Labsys TM TG-DSC16
Fig. :
12-05-12
Experiment : 3 Sn91 Zn6 Cd 3 cod no.4860/12
Procedure : 3 Sn91 Zn6 Cd3 cod no.4860/12 (Seq 3)
Atm. : argon
Crucible : Al2O3 100
Mass (mg) : 20.0
Heat Flow/ µV
Exo
Onset point : 64.51 °C
Peak 1 top : 79.36 °C
Peak 2 top : 80.61 °C
Enthalpy / µV.s/mg : 1.6426 (Endothermic effect) (0.7828 + 0.8598)
Onset point : 156.48 °C
Peak 1 top : 159.47 °C
Peak 2 top : 159.63 °C
Enthalpy / µV.s/mg : 0.0309 (Endothermic effect) (0.0173 + 0.0136)
Onset point : 189.66 °C
Peak 1 top : 191.05 °C
Peak 2 top : 191.88 °C
Enthalpy / µV.s/mg : 0.0917 (Endothermic effect) (0.0745 + 0.0172)
Onset point : 194.63 °C
Peak 1 top : 197.49 °C
Peak 2 top : 197.57 °C
Enthalpy / µV.s/mg : 5.5652 (Endothermic effect) (1.7274 + 3.8378)
Temperature/ °C

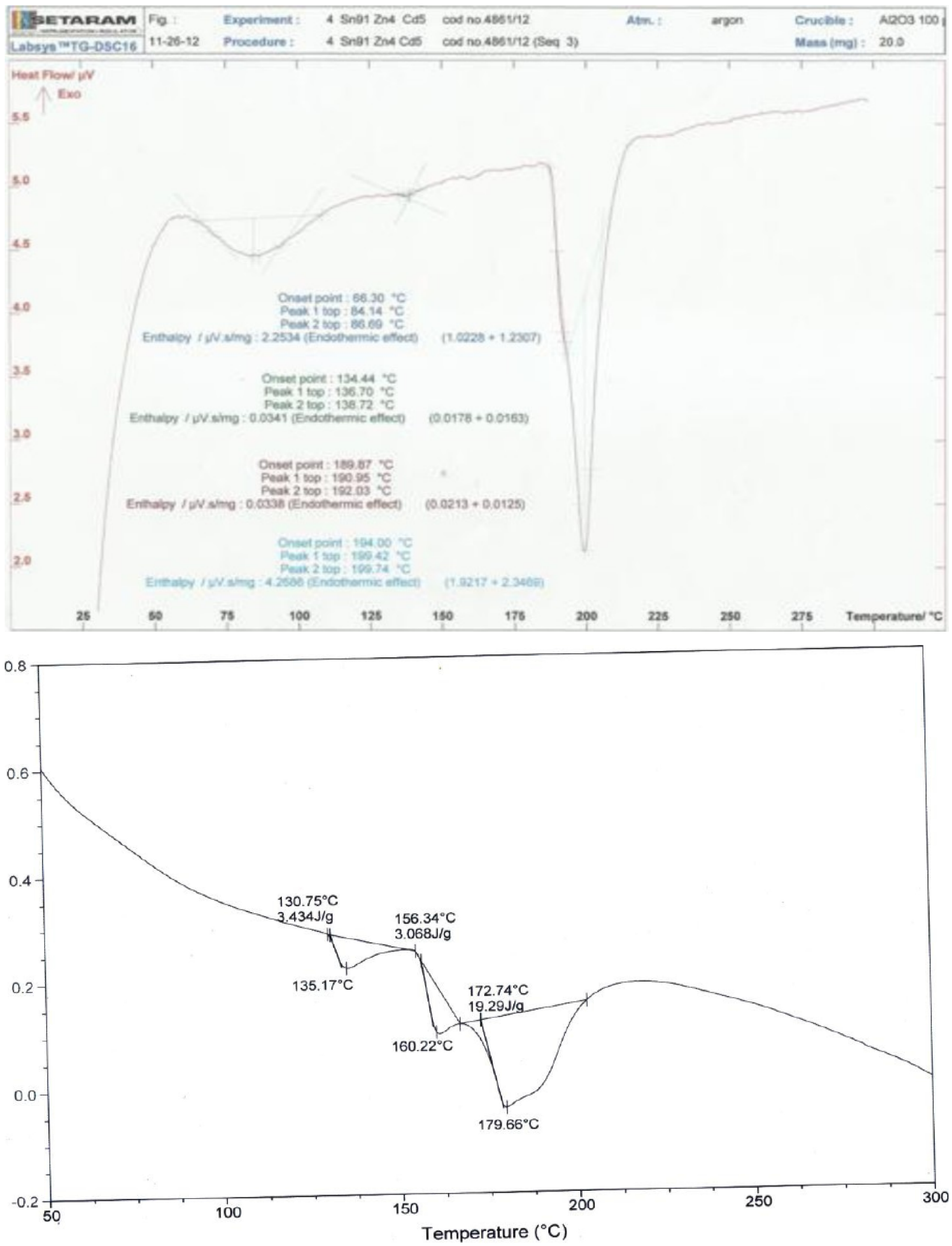

Figure 2 : DSC graphs of Sn-Zn-Cd rapidly solidified alloys

the temperature is increased during the scan. The pasty range is the difference between solidus and liquidus points which is seen in TABLE 3. The pasty range value of Sn- Zn alloy varied after adding cadmium content.

Electrical resistivity

Electrical resistivity value of Sn- Zn alloy is increased after adding cadmium content as seen in TABLE 4. That is because cadmium atoms is dissolved in the Sn- Zn matrix playing as the scattering center for conduction electrons/or changed matrix structure which increases their resistivity.

Elastic properties

Elastic modulus Sn- Zn alloy is decreased by add-

TABLE 4 : Electrical resistivity of quenched $Sn_{91}Zn_{9-x}Cd_x$ (x= 0, 1.5, 3, 5 wt.%) and $Sn_{86}Zn_4Cd_{10}$ alloys

Alloys	ρ x 10^{-8} (Ω.m)
$Sn_{91}Zn_9$	43.5±3.19
$Sn_{91}Zn_{7.5}Cd_{1.5}$	48.6±4.92
$Sn_{91}Zn_6Cd_3$	50.4±5.43
$Sn_{91}Zn_4Cd5$	59.7±5.72
$Sn_{86}Zn_4Cd_{10}$	64.9±6.42

TABLE 5 : Elastic modulus of quenched $Sn_{91}Zn_{9-x}Cd_x$ (x= 0, 1.5, 3, 5 wt.%) and $Sn_{86}Zn_4Cd_{10}$ alloys

Alloys	Elastic modulus (E) Gpa
$Sn_{91}Zn_9$	28.042±0.434
$Sn_{91}Zn_{7.5}Cd_{1.5}$	26.383±0.411
$Sn_{91}Zn_6Cd_3$	23.35±0.206
$Sn_{91}Zn_4Cd5$	20.753±0.575
$Sn_{86}Zn_4Cd_{10}$	22.996±0.088

ing cadmium content as shown in TABLE 5. That is because the dissolved Cadmium atoms on grain boundary/ or formed in Sn- Zn matrix affecting on bond matrix which decreasing elastic modulus of Sn- Zn alloy.

The resonance curves of $Sn_{91}Zn_{9-x}Cd_x$ (x= 0, 1.5, 3, 5 wt.%) and $Sn_{86}Zn_4Cd_{10}$ alloys are shown in Figure 3. Calculated Internal friction and thermal diffusivity values are seen in TABLE 6. The results show that, internal friction value of Sn-Zn alloy decreased by adding cadmium content but thermal diffusivity value is varied.

TABLE 6 : Internal friction and thermal diffusivity $Sn_{91}Zn_{9-x}Cd_x$ (x= 0, 1.5, 3, 5 wt.%) and $Sn_{86}Zn_4Cd_{10}$ alloys

Alloys	Internal friction (Q^{-1})	Thermal diffusivity (D_{th}) x 10^{-4} cm^2/sec
$Sn_{91}Zn_9$	0.273	1.282
$Sn_{91}Zn_{7.5}Cd_{1.5}$	0.302	1.562
$Sn_{91}Zn_6Cd_3$	0.324	1.694
$Sn_{91}Zn_4Cd5$	0.456	5.179
$Sn_{86}Zn_4Cd_{10}$	0.462	1.397

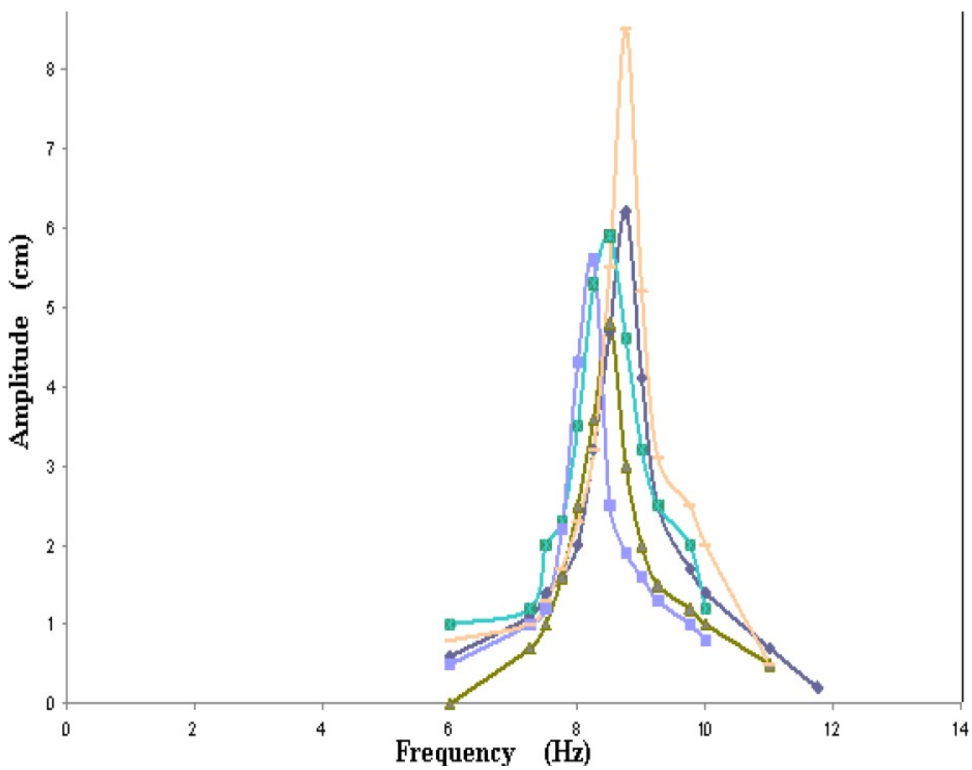

Figure 3 : Amplitude versus frequency of Sn-Zn-Cd alloys

CONCLUSION

Adding cadmium content caused change in Sn- Zn microstructure such as crystallinity and crystal size. Elastic modulus, internal friction and melting point values of Sn- Zn alloy decreased but electrical resistivity value increased after adding cadmium content to it. Also contact angle, Pasty range and thermal diffusivity values of Sn- Zn alloy varied after adding cadmium content to it.

$Sn_{86}Zn_4Cd_{10}$ alloy has best soldering properties for electronic applications.

REFERENCES

[1] R.K.Shiue, L.W.Tsay, C.L.Lin, J.L.Ou; J.Mater.Sci., **38**, 1269 **(2003)**.

[2] A.Miiyamoto, T.Ogawa, T.Ohsawa; Mater.Sci.Res.Inter., **9**, 16 **(2003)**.

[3] B.El-Bediwi, M.El-Sayed, M.Kamal; Radiation Effects & Defects in Solids, **160(7)**, 297–300 **(2005)**.

[4] T.Ohoka, Y.Nakamura, T.Ono; J.Mater.Sci., **39**, 4379-4381 **(2004)**.

[5] M.Mc Cormack, S.Jin, G.W.Kammlott, H.S.Chen, Appl.Phys.Lett., **63**, 15 **(1993)**.

[6] Y.L.Tsai, W.S.Hwang; Material Science and Engineering A, **413,414,** 312-316 **(2005)**.

[7] J.Glazer; J.Electron.Mater, **23**, 693-700 **(1994)**.

[8] Y.Kariya, M.Otsuka; J.Electron.Mater, **27**, 866-70 **(1998)**.

[9] W.J.Tomlinson, A.Fullylove; J.Mater.Sci., **27**, 5777-81 **(1992)**.

[10] F.Ochoa, J.J.Williams, N.Chawla; J.Electron Mater, **32**, 1414-20 **(2003)**.

[11] M.Mc Cormack, S.Jin; JOM., **45**, 38 **(1993)**.

[12] K.Kanlayasiri, M.Mongkolwongrojn, T.Ariga; Journal of alloys and compounds, **485**, 225-230 **(2009)**.

[13] A.El-Bediwi, M.M.El-Bahay; Radiation Effects & Defects in Solids, **159**, 133-40 **(2004)**.

[14] E.Schreiber, O.L.Anderson, N.Soga; Elastic constant and their measurements, McGraw-Hill, New York, 82 **(1973)**.

[15] S.Timoshenko, J.N.Goddier; Theory of elasticity, 2nd Edition, McGraw-Hill, NewYork, 277 **(1951)**.

[16] K.Nuttall; J.Inst.Met., **99**, 266 **(1971)**.